Micron 88 (2016) 48–53

Contents lists available at ScienceDirect

Micron

journal homepage: www.elsevier.com/locate/micron

Te inclusion-induced electrical field perturbation in CdZnTe single crystals revealed by Kelvin probe force microscopy

Yaxu Gu[a,b], Wanqi Jie[a,b,*], Linglong Li[c], Yadong Xu[a,b,*], Yaodong Yang[c], Jie Ren[a], Gangqiang Zha[a,b], Tao Wang[a,b], Lingyan Xu[a,b], Yihui He[a,b], Shouzhi Xi[a,b]

[a] State Key Laboratory of Solidification Processing, School of Materials Science and Engineering, Northwestern Polytechnical University, Xi'an 710072, PR China
[b] Key Laboratory of Radiation Detection Materials and Devices of Ministry of Industry and Information Technology, Northwestern Polytechnical University, Xi'an 710072, PR China
[c] Multidisciplinary Material Research Center, Frontier Institute of Science and Technology, Xi'an Jiaotong University, Xi'an 710049, PR China

ARTICLE INFO

Article history:
Received 17 May 2016
Received in revised form 10 June 2016
Accepted 10 June 2016
Available online 16 June 2016

Keywords:
CdZnTe
Te inclusion
Kelvin probe force microscopy
Electrical property
Bias dependent

ABSTRACT

To understand the effects of tellurium (Te) inclusions on the device performance of CdZnTe radiation detectors, the perturbation of the electrical field in and around Te inclusions was studied in CdZnTe single crystals via Kelvin probe force microscopy (KPFM). Te inclusions were proved to act as lower potential centers with respect to surrounding CdZnTe matrix. Based on the KPFM results, the energy band diagram at the Te/CdZnTe interface was established, and the bias-dependent effects of Te inclusion on carrier transportation is discussed.

1. Introduction

II–VI compound semiconductors, CdTe and CdZnTe (CZT), have been widely used for hard X- and gamma-ray detection (Franc et al., 1999). Melt growth under a slight excess of tellurium is often adopted to grow high resistivity CdTe and CdZnTe ingots by forming Te antisites (Lindström et al., 2016). However, one of the limitations of this method is the trapping of Te-rich droplets by the growth interface (Rudolph et al., 1995). Therefore, Te inclusions, usually in the size of 1–50 μm, exist prevalently in the as-grown crystals. Much attention has been devoted to the influence of Te inclusions on the local carrier transport properties both experimentally (Carini et al., 2007) and numerically (Bolotnikov et al., 2007a). Te inclusions were found to reduce the local charge collection efficiency (CCE) (Amman et al., 2002), and thus to degrade the energy resolution of CdZnTe radiation detectors (Bolotnikov et al., 2007b). For example, Carini et al. (Carini et al., 2006) and Hansson et al. (Hansson et al., 2012) observed a clear one to one correspondence between the low CCE regions and the location of Te inclusion using X-ray response mapping. Bolotnikov et al. (Bolotnikov et al., 2007c) proposed a geometry model to explain charge loss induced by Te inclusion, and simulated the effects of size and density of Te inclusions on gamma-ray spectra. Bale (Bale, 2010) further modeled the cumulative effect of Te inclusions in CdZnTe radiation defectors. A noticeable temperature-dependent influence of Te inclusions on charge collection was observed and attributed to polarization effect by Hossain et al. (Hossain et al., 2011). Even though progress has been made on understanding the role of Te inclusions, little is known on the electrical behaviors of Te inclusions in CdZnTe crystals. Since electrical field plays an important role in the charge collection property of radiation-generated carriers (Cola and Farella, 2013), revealing the effect of Te inclusions on the electrical field is therefore of importance to optimize the operation properties of CdZnTe detectors. Besides, it may also advance the knowledge of nanoscale Te precipitates (Rudolph et al., 1993) and other inclusions in corresponding devices, e.g., indium inclusions in InN (Liu et al., 2012) and carbon inclusions in GaN (Lefeld-Sosnowska and Frymark, 2001).

In this work, Te inclusion-induced electrical property variation in CdZnTe single crystals is studied via KPFM. The measured potential distribution in and around Te inclusions is analyzed

* Corresponding authors at: State Key Laboratory of Solidification Processing, School of Materials Science and Engineering, Northwestern Polytechnical University, Xi'an 710072, PR China.
E-mail addresses: jwq@nwpu.edu.cn (W. Jie), xyd220@nwpu.edu.cn (Y. Xu).

http://dx.doi.org/10.1016/j.micron.2016.06.001
0968-4328/

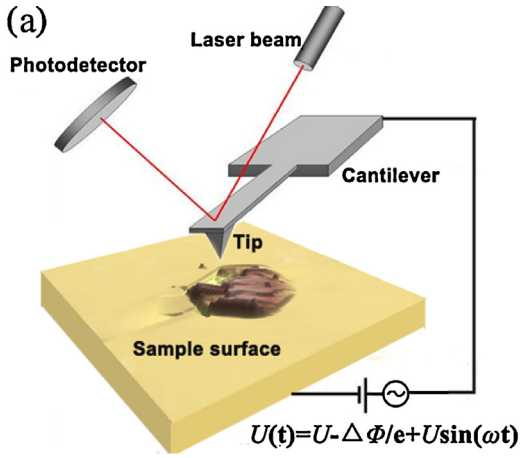

Fig. 1. Schematic diagram of KPFM scanning over a Te inclusion embedded on cleaved (110) CdZnTe surface.

by employing the Poisson's equation, and possible carrier transportation across Te inclusion is discussed. Based on KPFM results, electrical potential distribution around Te inclusions under different biases are numerically simulated using the software COMSOL Multiphysics 4.3a.

2. Experimental

$Cd_{0.9}Zn_{0.1}Te$: In single crystals grown by modified vertical Bridgman method in Imdetek were used in the experiments. The effective doping level of In in the as-grown ingot is about 30 ppm. To avoid the influence of surface contamination on KPFM results, CdZnTe samples were kept in nitrogen atmosphere immediately after cleavage in clear and dry air. KPFM measurements were carried out on a commercial AFM platform (Asylum, Cypher S) as illustrated in Fig. 1. Te inclusion with a flat cross-section was observed on the cleaved (110) CdZnTe surface, which meets the requirement of surface evenness of KPFM test and subsequent interfacial analysis. Since (110) CdZnTe surface is electrically neutral and is free of charged states, the influence of surface dipole as well as charged adsorbate on the measured potential distribution can therefore be minimized. Frequency modulation (FM) mode was used in KPFM measurements to achieve high spatial resolution. The lift height of Ti/Ir-coated Si probe was set to be about 20 nm, and the applied ac voltage was 800 mV in all experiments. Potential fluctuation caused by systematic noise is below 0.50 mV, and the vertical noise floor in Z direction is less than 15 pm. Fig. 2(a) and (b) shows the topography and surface potential (or Kelvin potential) in and around a Te inclusion on the cleaved (110) CdZnTe surface, respectively. The root-mean-square roughness of CdZnTe surface in Fig. 2(a) is about 0.14 nm.

3. Results and discussion

3.1. Electrical potential distribution at Te/CdZnTe interface

Corresponding to the topography of Te inclusion shown in Fig. 2(a), surface potential distribution is obtained with KPFM (Fig. 2(b)), which demonstrates that Te inclusions act as lower potential centers in CdZnTe crystal. According to the results of Gaussian fitting to the histogram of pixel potentials in Fig. 2(b), the potential of Te inclusion is about 0.32 V lower than that of CdZnTe matrix. Moreover, the low potential region around the Te inclusion extends into CdZnTe matrix for several μm. This electrical field inhomogeneity will expectedly cause a fluctuation of electron drift velocity, and further deteriorate the imaging performance in pixelated detectors (Kim et al., 2011).

Fig. 2(c) and (d) shows the topography and potential profile along the dotted line in Fig. 2(b). The dotted line is chosen perpendicular to the Te/CdZnTe boundary. According to the tetrakaidecahedron model on the morphology evolution of Te inclusions (He et al., 2012), Te inclusions are embodied with oriented CdZnTe planes, preferentially with the orientations $\{01\bar{1}1\}_{Te}\|\{111\}_{CdZnTe}$ and $\{0001\}_{Te}\|\{100\}_{CdZnTe}$. Since CdZnTe lattice is body-centred cubic, the cleaved (110) CdZnTe surface or Te cross-section is thus perpendicular to corresponding intersecting Te/CdZnTe interfaces. Therefore, the dotted line is perpendicular to the intersecting Te/CdZnTe interface, which is beneficial to employ one-dimensional approximation in the analysis of Te/CdZnTe interface. To fully understand Te/CdZnTe interfacial electrical properties, such as electrical field and space charge density distribution, the potential profile in Fig. 2(d) are further analyzed by solving the one-dimensional Poisson's equation. Due to the influence of surface undulation (Li and Li, 2005), however, potential profile within Te inclusion fluctuates substantially, which introduces significant noise to the calculated electrical properties. In order to suppress the influence of this unreasonable potential fluctuation on the calculated electrical field and the space-charge distribution, the Savitzky-Golay (SG) smoothing (Luo et al., 2005) with the even number $m = 7$, polynomial of degree $p = 2$ and differential order $d = 0$ was performed on the measured potential profile in Fig. 2(d). The smoothed potential profile is shown by the dotted line in Fig. 2(d). Given the dielectric constants $\varepsilon_{CZT} = 10.4$ (Li et al., 2012), $\varepsilon_{Te} = 30.0$ (Madelung, 1996) and $\varepsilon_0 = 8.9 \times 10^{-14}$ F cm^{-1}, the calculated electrical field and space-charge density profile are obtained (see Fig. 2(e)–(f)).

Fig. 2(e) shows that the electrical field reaches up to its maximum of about 2000 V cm^{-1} at Te/CdZnTe interface. The calculated space-charge distribution suggests that high density of positive space charge exists in CdZnTe crystals, while negative space charge accumulates at Te inclusion side (see Fig. 2(f)). The space-charge density in CdZnTe matrix reaches up to 6×10^{12} $q_0 \cdot cm^{-3}$ at 5 μm and 13.5 μm in X axis, with the elementary charge q_0. This value is about 2–3 orders of magnitude higher than the fully-depleted CdZnTe bulk crystals measured using transient current technique by Uxa et al. (Uxa et al., 2012) or the results of Pockels electro-optical technique by Sellin and Franc et al. (Franc et al., 2011; Sellin et al., 2010), which indicates a higher density of defects in the region surrounding Te inclusions.

3.2. Energy band diagram and proposed carrier transport process across Te/CdZnTe interface

The surface potential obtained from KPFM presents the variation of local vacuum level (Cahen and Kahn, 2003). Since the electron affinity stays constant for a given surface, the measured potential distribution thus further predicts the energy band alignment of the regions investigated. The change of local vacuum level E_{vac}, usually expressed as qV_{bi}, corresponds to the variation of potential profile in Fig. 2(d). Furthermore, the potential difference is mainly distributed near Te/CdZnTe boundary, and thus the band bending across the interface can be determined accordingly, which provides guidance for understanding the negative effects of Te inclusions. A qualitative energy band diagram across Te/CdZnTe interface (Fig. 3(a)) is proposed based on the potential profile shown in Fig. 2(d).

As seen in Fig. 3(a), a downward band bending from the interface to CdZnTe crystals acts as a potential well for holes, which demonstrates that severe hole trapping can be caused by Te inclusions (Bolotnikov et al., 2009). Besides, X-ray response